Cell, Vol. 104, 57–69, January 12, 2001, Copyright ©2001 by Cell Press

The Cytoplasmic Domain of the Ligand EphrinB2 Is Required for Vascular Morphogenesis but Not Cranial Neural Crest Migration

Ralf H. Adams,*§ Francesca Diella,* Silvia Hennig,† Françoise Helmbacher,* Urban Deutsch,† and Rüdiger Klein*‡

*European Molecular Biology Laboratory
Meyerhofstrasse 1
D-69117 Heidelberg
Germany

†Max-Planck-Institute for Physiological and Clinical Research
W.G. Kerckhoff Institute
Bad Nauheim
Germany

Summary

The transmembrane ligand ephrinB2 and its cognate Eph receptor tyrosine kinases are important regulators of vascular morphogenesis. EphrinB2 may have an active signaling role, resulting in bi-directional signal transduction downstream of both ephrinB2 and Eph receptors. To separate the ligand and receptor-like functions of ephrinB2 in mice, we replaced the endogenous gene by cDNAs encoding either carboxy-terminally truncated (ephrinB2$^{\Delta C}$) or, as a control, full-length ligand (ephrinB2^{WT}). While homozygous *ephrinB2*$^{WT/WT}$ animals were viable and fertile, loss of the ephrinB2 cytoplasmic domain resulted in midgestation lethality similar to *ephrinB2* null mutants (ephrinB2^{KO}). The truncated ligand was sufficient to restore guidance of migrating cranial neural crest cells, but ephrinB2$^{\Delta C/\Delta C}$ embryos showed defects in vasculogenesis and angiogenesis very similar to those observed in ephrinB2$^{KO/KO}$ animals. Our results indicate distinct requirements of functions mediated by the ephrinB carboxyterminus for developmental processes in the vertebrate embryo.

Introduction

Morphogenesis in the embryo is controlled by signals from the cellular environment, generated as a result of patterning processes at work in the early embryo. Eph receptors and their ligands, the ephrins, appear to lie functionally at the interface between patterning and morphogenesis, because they regulate many of the dynamic changes that occur during this embryonic phase, including cell migration, axon guidance, and angiogenesis (reviewed in Holder and Klein, 1999; Gale and Yancopoulos, 1999; Wilkinson, 2000). The Eph receptor family is part of the large superfamily of receptor tyrosine kinases and is subdivided into two structurally distinct subclasses, which differ in their ligand binding specificities. EphA receptors bind to glycosylphosphatidylanchored ephrinA ligands, whereas EphB receptors (and EphA4) bind to ephrinB ligands, transmembrane proteins carrying a highly conserved 80 residue cytoplasmic domain. (reviewed in Flanagan and Vanderhaeghen, 1998; Wilkinson, 2000).

Recent work in the mouse has demonstrated important roles for ephrinB2 and its cognate EphB receptors in vascular development. Reciprocal expression of ephrinB2 and EphB4 in arterial and venous endothelial cells, respectively, suggested ephrinB2-EphB4 interactions at the arterial–venous interface (Wang et al., 1998; Adams et al., 1999; Gerety et al., 1999). Consistently, knockout mice lacking either ephrinB2 or EphB4 die during embryogenesis and display similar cardiovascular defects (Wang et al., 1998; Gerety et al., 1999). Angiogenic remodeling in yolk sac and embryos was defective, resulting in arrest at the primitive capillary plexus stage. Partially penetrant defects in large vessel primordia of the embryo demonstrated a requirement for ephrinB2 in some aspects of vasculogenesis (Adams et al., 1999). Interactions between ephrinB ligands and EphB receptors away from the arterial–venous interface were suggested by overlapping expression of ephrinB1 ligand and EphB3 and EphB4 receptors on venous endothelial cells. Moreover, mesenchymal cells adjacent to blood vessels were found to express EphB2 receptors, and somitic ephrinB ligands were in direct contact to EphB receptors on intersomitic vessels. Functional relevance of these interactions was demonstrated by partially penetrant vascular defects in *ephB2*/*ephB3* double homozygous embryos (Adams et al., 1999).

Whereas the mechanism of ephrin/Eph signaling in the vasculature is presently not understood, in the developing nervous system, ephrins are repulsive guidance cues for navigating neuronal growth cones and migrating neural crest cells (reviewed in Holder and Klein, 1999; Wilkinson, 2000). Neural crest cells delaminate from the dorsolateral edge of the neural tube and migrate along specific pathways to various destinations where they differentiate into many different cell types, including neurons and glia of the peripheral nervous system, connective and skeletal tissue of the head, and melanocytes of the skin. In the head region, neural crest cells delaminate from the segmented hindbrain and migrate as segmental streams into the branchial arches (Kontges and Lumsden, 1996). In *Xenopus* embryos, ephrinB2 and its cognate receptors EphB1 and EphA4 are expressed in adjacent neural crest streams and underlying mesoderm. Overexpression of either dominant-negative Eph receptors or wild-type ephrinB2 caused aberrant migration of crest cells, presumably because the expression of repulsive guidance cues had been altered (Smith et al., 1997). Similarly, migration of trunk neural crest cells, which express EphB receptors, is guided in vitro by repulsive ephrinB ligands expressed in posterior half somites (Krull et al., 1997; Wang and Anderson, 1997). These studies provided compelling evidence for a role of ephrin/Eph signaling in neural crest migration, although corroborating data from genetic loss-of-function analyses were still missing.

‡To whom correspondence should be addressed (e-mail: klein@embl-heidelberg.de).
§Present address: Imperial Cancer Research Fund, London WC2A 3PX, United Kingdom.

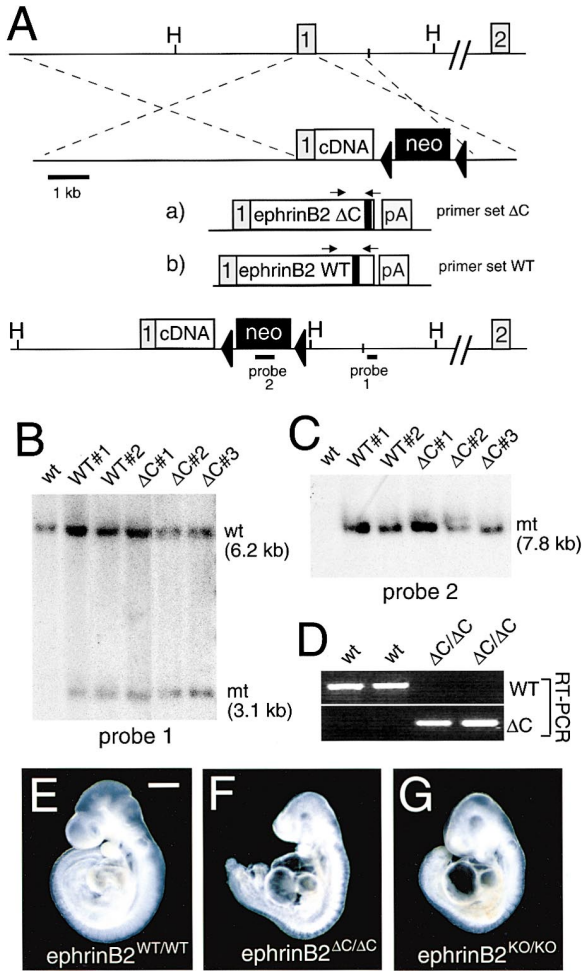

Figure 1. Generation of *ephrinB2* cDNA Knockin Mutants

(A) Schematic representation of the mouse *ephrinB2* gene with the first exon (gray box) that contains the 5′ end of the open reading frame. cDNAs (white boxes), encoding either (a) carboxyterminally truncated ephrinB2$^{\Delta C}$ or (b) full-length ephrinB2^{WT} ligand were fused in frame with the first exon and thereby placed under control of the endogenous gene promoter. The transmembrane region (black box) and the following 14 amino acid residues were preserved in ephrinB2$^{\Delta C}$ protein. A hemagglutinin (HA) epitope tag was fused to the ephrinB2$^{\Delta C}$ carboxyterminus for protein detection (not shown). A loxP-flanked (black triangles) neomycin selection marker (black box) was used for subsequent removal by the Cre recombinase (not shown). HindIII restriction sites ("H"), probes used for Southern hybridization, and primer sets for RT-PCR (ΔC, WT) are indicated.

(B) Homologous recombination was verified by Southern hybridization with ES cell genomic DNA following enzymatic restriction by HindIII. Probe 1, corresponding to intronic sequences adjacent to the 3′ end of the targeted region, detected a 6.2 kb DNA fragment for the wild-type allele both in untransfected (wt) and clones of transfected ephrinB2^{WT} (WT#1,2) or ephrinB2$^{\Delta C}$ (ΔC#1, 2, 3) ES cells. The 3.1 kb DNA fragment corresponding to the targeted allele was only present in transfected cells.

(C) The neomycin resistance–specific probe 2 labeled a 7.8 kb HindIII DNA fragment only in ES cell clones after homologous recombination at the gene locus.

(D) mRNA encoding the ephrinB2 cytoplasmic domain was detectable by RT-PCR (primer set WT indicated in [A]) in E9.5 wild-type embryos but not in *ephrinB2*$^{\Delta C/\Delta C}$ homozygotes. PCR amplification with an HA tag–specific antisense oligo (set ΔC) yielded a product exclusively from ephrinB2$^{\Delta C}$ RNA. Neither amplification product was obtained from *ephrinB*$^{KO/KO}$ embryos (not shown).

Increasing evidence suggests that transmembrane ephrin ligands have intrinsic signaling capability. Thus, cell contact–induced interaction between ephrinB ligands and Eph receptors can trigger bidirectional signals into both cells, via classical forward signaling mediated by the tyrosine kinase domain of the Eph receptor and via nonconventional reverse signaling mediated by the ephrinB cytoplasmic domain (reviewed in Holder and Klein, 1999; Wilkinson, 2000). Soluble artificially clustered EphB ectodomains induce rapid phosphorylation of conserved tyrosine residues in the cytoplasmic part of ephrinB molecules, thereby presumably creating docking sites for phosphotyrosine binding proteins. Moreover, ephrinB ligands and Eph receptors carry conserved carboxyterminal binding motifs for PDZ domain–containing proteins, which might have roles in cell surface localization, clustering, and/or signaling (reviewed in Holder and Klein, 1999; Wilkinson, 2000). Ephrins are localized in lipid raft microdomains, which are sites of interaction with PDZ-domain proteins and the Fyn tyrosine kinase (Brückner et al., 1999; Davy et al., 1999). EphB2 receptors are required for the formation of the anterior commissure (AC), a forebrain axon tract (Henkemeyer et al., 1996). To exert this function, EphB2 receptors do not require an active kinase domain and may induce ephrinB reverse signaling in AC axons (Henkemeyer et al., 1996). More recently, ephrin reverse signaling was shown to be sufficient for cell sorting at hindbrain segment boundaries in the Zebrafish embryo and bidirectional signaling restricted cell intermingling in the fish animal cap assay (Mellitzer et al., 1999; Xu et al., 1999).

Here, we describe the phenotype of knockin mutant mice in which endogenous ephrinB2 was replaced by mutant ephrinB2 lacking its cytoplasmic part (ephrinB2$^{\Delta C}$). EphrinB2$^{\Delta C}$ is functionally restricted to induce forward signaling by Eph receptors on adjacent cells, but is no longer able to exert reverse signaling via its cytoplasmic domain. We demonstrate that ephrinB2$^{\Delta C}$ mediates branchial arch morphogenesis and aortic arch formation by guiding migrating neural crest cells. In this process, ephrinB2 serves primarily as a ligand for Eph receptors expressed in neural crest cells. In contrast, angiogenic remodeling and the formation of major embryonic vessels by vasculogenesis require full-length ephrinB2, suggesting that the ephrinB2 cytoplasmic domain and reverse signaling are essential in vascular cells.

Results

Generation of Mutant Mice Expressing Truncated EphrinB2

To study the function of the ephrinB2 cytoplasmic domain in vivo, we targeted the mouse *ephrinB2* gene and inserted a cDNA encoding either full-length wild-type (ephrinB2^{WT}) or truncated ephrinB2 (ephrinB2$^{\Delta C}$), in

(E–G) Appearance of freshly dissected homozygous *ephrinB2* mutant embryos at E9.5. No morphological differences were seen between *ephrinB2*$^{WT/WT}$ (E) and wild-type littermates (not shown). In contrast, *ephrinB2*$^{\Delta C/\Delta C}$ mutants (F) displayed growth retardation and enlarged hearts as previously described for *ephrinB2*$^{KO/KO}$ animals (G). Scale bar in E is 400 μm in E, F, and G.

which 66 amino acid residues of the carboxyterminus were replaced by a hemagglutinin (HA) epitope tag (Figure 1A). Using standard gene targeting technology (Figures 1B and 1C), a mouse line was established for each of the targeted cDNA insertions, *ephrinB2*^{WT} and *ephrinB2*$^{\Delta C}$. The *neo* selection cassette was subsequently removed by crossing heterozygous mutant mice with a deleter-cre line. The *cre* allele was removed by backcrossing to C57BL/6 wild-type animals so that mutants expressed neither Cre recombinase nor neomycin resistance. Both mutants (*ephrinB2*$^{WT/WT}$ and *ephrinB2*$^{\Delta C/\Delta C}$) and *ephrinB2* knockout mice (Adams et al., 1999) were analyzed in similar mixed C57BL/6 × 129svev backgrounds to allow direct comparison. Interbreeding of *ephrinB2*^{WT} heterozygous animals yielded viable, healthy, and fertile homozygous offspring at Mendelian ratios indicating that no detrimental defects were caused by the targeting procedure and the switch to cDNA expression itself. In contrast, homozygous *ephrinB2*$^{\Delta C/\Delta C}$ mice were found to be embryonic lethal at midgestation (E10.5–E11) already exhibiting general growth retardation and inflation of the pericard highly reminiscent of the *ephrinB2* knockout phenotype at E9.5 (Figures 1F and 1G). Again, freshly dissected *ephrinB2*$^{WT/WT}$ embryos (Figure 1E) displayed no growth retardation or developmental defects and were indistinguishable from control *ephrinB2*$^{WT/+}$ or wild-type littermates (not shown).

The EphrinB2 Cytoplasmic Domain Is Not Essential for Cell Surface Localization and Eph Receptor Activation

To exclude that severe defects of *ephrinB2*$^{\Delta C/\Delta C}$ mutants were due to lack of expression from the knockin allele, we investigated expression of the truncated transmembrane ligand in mouse embryos. By in situ hybridization with an antisense RNA probe, expression of ephrinB2 was easily detectable in forebrain, hindbrain, branchial arches, dorsal aorta, and aortic arches of E9.5 (18–25 somites) wild-type animals (Figure 2A). Very similar expression patterns and levels were seen in *ephrinB2*$^{WT/WT}$ and *ephrinB2*$^{\Delta C/\Delta C}$ mutants, whereas no signal above background levels was detected in *ephrinB2* knockout embryos (Figures 2B–2D). We used a fusion of the aminoterminal EphB4 receptor ectodomain and alkaline phosphatase (EphB4-AP) to detect ephrinB2 protein, which appears to be the only known ligand for this receptor (Wilkinson, 2000). Specific staining in E9.5 wild-type embryos was most prominent in hindbrain and branchial arches (Figure 2E) and completely absent in *ephrinB2* null mutants (Figure 2H). Specific staining was also seen in hindbrain and branchial arches of both homozygous *ephrinB2*$^{WT/WT}$ and *ephrinB2*$^{\Delta C/\Delta C}$ mutants, indicating that the cDNA encoded ligand protein is available at the cell surface of the embryos where it can be recognized by the corresponding receptors (Figures 2F and 2G).

EphrinB2 protein can be detected in embryo lysates by immunoblotting with an anti-ephrinB2 antibody after pull down with wheat germ agglutinin (WGA), a lectin that binds the N-acetyl-β-D-glucosamyl residues of glycosylated cell surface proteins. Although numerous bands of different molecular weights were recognized by this procedure, ephrinB2 was identified as several protein isoforms of about 40–45 kDa by its absence in null embryos (Figure 2I). Likewise, epitope-tagged ephrinB2$^{\Delta C}$ was detectable as 2–3 isoforms with an apparent molecular weight of 35–40 kDa using an anti-HA antibody. The intensities of full length and truncated ephrinB2 in *ephrinB2*$^{WT/\Delta C}$ double heterozygous embryos appeared to be similar excluding the possibility that the phenotype of *ephrinB2*$^{\Delta C/\Delta C}$ mutants was due to poor expression of ephrinB2$^{\Delta C}$ protein (Figure 2J).

Ectopic expression of carboxyterminally truncated ephrinB2 protein had previously been shown to induce autophosphorylation of its cognate EphA4 receptor in zebrafish hindbrain cells (Xu et al., 1999). We wanted to test whether ephrinB2$^{\Delta C}$ protein was also able to activate endogenous EphB4 receptors in primary endothelial cells. We expressed either ephrinB2^{WT} or ephrinB2$^{\Delta C}$ in HEK293 cells and obtained membrane preparations of transfected cells to stimulate EphB4 receptors on cultured human umbilical vein endothelial cells (HUVECs). Similar levels of EphB4 receptor tyrosine phosphorylation were observed with ephrinB2^{WT}- and ephrinB2$^{\Delta C}$-containing membranes, whereas membranes from mock-transfected cells did not induce EphB4 autophosphorylation over background levels (Figure 2K). This result confirmed the ability of ephrinB2 to activate its receptor on adjacent cells independent of the ligand cytoplasmic domain.

Expression of EphrinB2 and Its Receptors in Branchial Arches and Cranial Neural Crest Cells

As shown in Figure 2, branchial arches are prominent sites of ephrinB2 expression in the early mouse embryo and branchial arch morphogenesis is defective in *ephrinB2* null mutants (see below). We therefore analyzed in more detail the expression of ephrinB2 and its receptors in branchial arches. By staining with EphB4-AP fusion protein, ephrinB2 protein was detected in the branchial arch region already at E8.5, where it was most pronounced in the cleft area between arches 1 and 2, a contact zone between surface ectoderm and foregut endoderm (Figure 3A). Sectioning identified surface ectoderm as the primary source of ephrinB2 (Figure 3B). Likewise, *ephrinB2* mRNA could be detected by in situ hybridization in branchial arch surface ectoderm and in adjacent mesenchymal cells in E9.5 embryos (Figure 3C). Ectoderm and gut endoderm form the pocket-like structure of the branchial arch that is subsequently populated by migrating mesodermal and cranial neural crest cells. In 15–25 somite stage embryos, these cell populations express multiple receptors for ephrinB2. EphA4 receptor, detected by a *lacZ* knockin allele (Helmbacher et al., 2000), was expressed on cells migrating to the second and third, but not to the first arch (Figures 3D and 3E). Similarly, in situ hybridization analysis with an *ephB3* antisense probe labeled cells migrating into all three arches (Figure 3H); signals for *ephB1* in the same area were present, but much weaker (Figure 3F). In contrast, we failed to see expression of EphB2lacZ fusion protein (Henkemeyer et al., 1996) on these cell streams (Figure 3G). Instead, EphB2 was expressed in the trigeminal ganglion (V) and the nervus vagus (VII), which are derived from a different neural crest cell population (Fig-

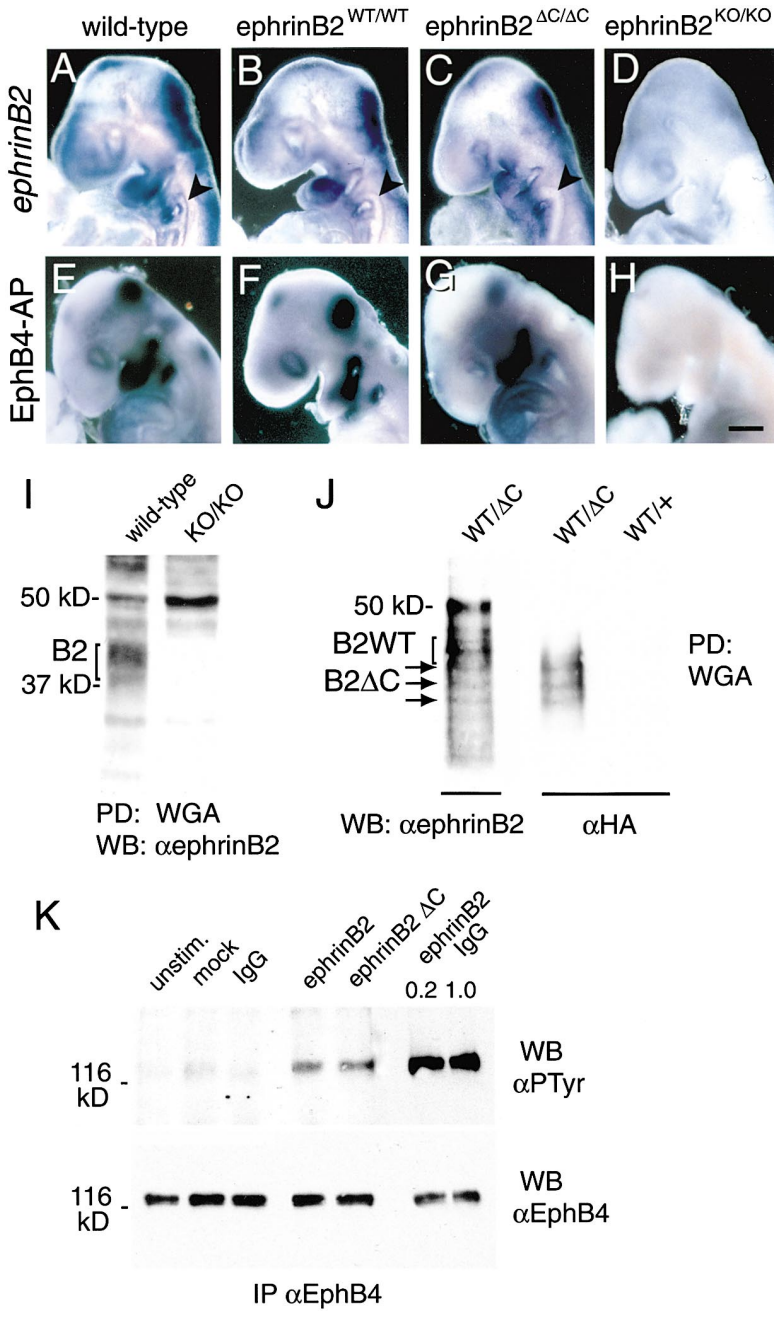

Figure 2. Expression of EphrinB2 in Mutant Embryos and EphB4 Receptor Activation

(A–D) Whole-mount in situ hybridization analysis of ephrinB2 mRNA and (E–H) staining with EphB4-AP receptor bodies for the detection of ephrinB2 protein in (A and E) wild-type, (B and F) *ephrinB2*$^{WT/WT}$, (C and G) *ephrinB2*$^{\Delta C/\Delta C}$, and (D and H) *ephrinB2*$^{KO/KO}$. The frontal part of E9.5 embryos (20–25 somites) are shown. An ephrinB2 antisense RNA probe specifically labeled hindbrain, branchial arches, aortic arch, and dorsal aorta (arrowheads) in wild-type control embryos (A). Similar patterns and intensities of signals were obtained for *ephrinB2*$^{WT/WT}$ and *ephrinB2*$^{\Delta C/\Delta C}$ homozygotes (B and C), but not for ephrinB2 knockout embryos (D). Alkaline phosphatase activity derived from the EphB4-AP fusion protein was detected in hindbrain and branchial arches of wild-type (E), *ephrinB2*$^{WT/WT}$ (F), and *ephrinB2*$^{\Delta C/\Delta C}$ (G), but not in *ephrinB2*$^{KO/KO}$ embryos (H). The complete lack of binding of EphB4-AP in ephrinB2 knockout embryos indicates the specificity of EphB4 toward ephrinB2.

(I) Glycosylated cell surface proteins from E9.5 wild-type or homozygous *ephrinB2*$^{KO/KO}$ embryos were enriched by pull down with wheat germ agglutinin (WGA). Endogenous ephrinB2 ligand (B2, 40–45 kDa) was detected by Western blotting with an antibody directed against the extracellular domain of the mouse protein. Note absence of specific bands in knockout embryos (KO/KO).

(J) Epitope-tagged ephrinB2$^{\Delta C}$ (B2ΔC, 35–40 kDa) expressed in E10.5 mutant animals was identified by WGA pull down and immunoblotting with an anti-HA antibody. The signal was absent in ephrinB2^{WT} heterozygotes (WT/+). EphrinB2$^{\Delta C}$ protein (doublet or triplet bands) was also recognized by anti-ephrinB2 antibody. Expression levels appeared similar to *ephrinB2*^{WT} full-length protein (B2WT) in double heterozygous *ephrinB2*$^{WT/\Delta C}$ mutants (WT/ΔC), though somewhat reduced in comparison to untargeted wild-type animals (not shown). Additional bands (>48 kDa and <35 kDa) were also seen in lysates from ephrinB2 KOs and thus were considered nonspecific.

(K) Endogenous EphB4 receptor expressed by primary human umbilical vein endothelial cells (HUVEC) was either left unstimulated, or stimulated with membrane extracts from 293 cells transfected with either empty vector (mock) or ephrinB2^{WT} and ephrinB2$^{\Delta C}$ expression constructs. Tyrosine phosphorylation was analyzed by Western blotting of immunoprecipitated EphB4 protein. Receptor activation by antibody-clustered ephrinB2-Fc (0.2 and 1 μg/ml) are shown as positive controls. A shorter exposure is shown. After stripping of the blot, levels of EphB4 receptor were immunodetected with αEphB4 antibody. Scale bar in (H) is 160 μm in (A)–(H).

ure 3G). These results indicated that at least three receptors, EphA4, EphB1, and EphB3, are expressed at the right time in cell populations, which migrate along a path outlined by ephrinB2-expressing cells.

In the dorsal neural tube, prominent *ephrinB2* expression was detected below emerging and migrating neural crest cells, identified by expression of cellular-retinoic-acid binding-protein 1 (crabp1; Maden et al., 1992), a marker for multiple streams of cranial neural crest cells (Figures 3I and 3J). As described above, ephrinB2 protein was also prominently seen in cleft surface ectoderm around its interface with foregut endoderm (Figure 3K). These ephrinB2-positive regions appeared to be avoided by cranial neural crest cells (Figure 3L). Indeed, sections of embryos stained by whole-mount in situ hybridization confirmed that *ephrinB2* and *crabp1* expression were mutually exclusive (Figures 3M and 3N).

Branchial Arch Defects in *ephrinB2* Null, but Not *ephrinB2*$^{\Delta C/\Delta C}$ Mutants

The prominent expression of ephrinB2 in branchial arches and its receptors on migrating cells in the cranial

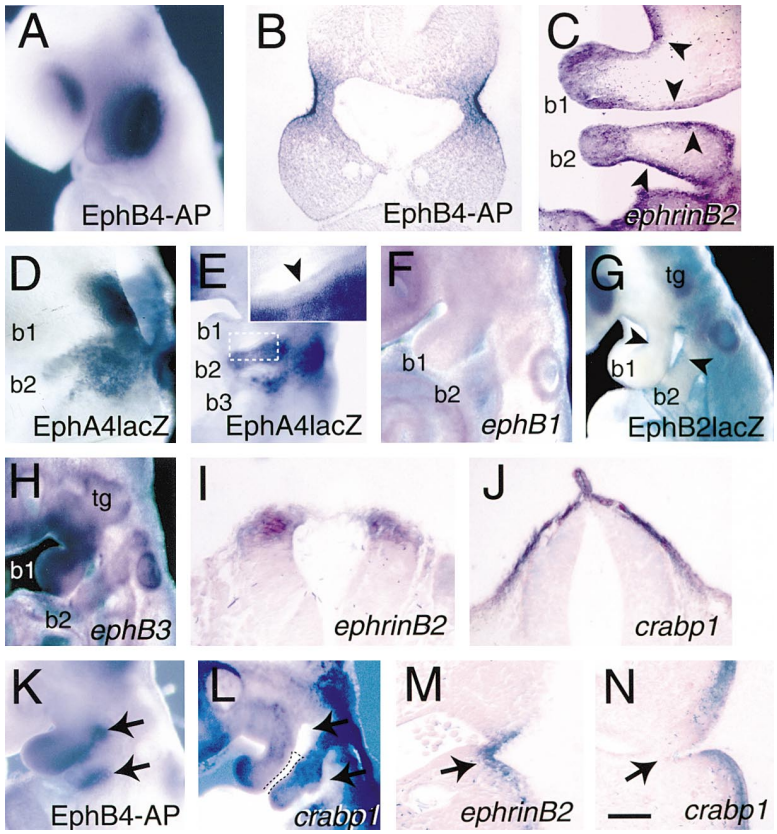

Figure 3. Expression of EphrinB2 and Its Cognate Eph Receptors in Branchial Arches and the Hindbrain Region

Whole-mount EphB4-AP staining (A, B, and K) or in situ hybridization analysis of wild-type embryos with (C, I, and M) ephrinB2, (F) EphB1, and (H) EphB3 antisense RNA probes. Embryonic stages shown are E8.5 (10–12 somites; A and B) or E9.5 (20–25 somites; C, F, and H–N). β-galactosidase stainings of heterozygous (D and E) EphA4lacZ and (G) EphB2lacZ knockins at E9.0 or E9.5 are shown. (A and B) E8.5, ephrinB2 expression is most prominent in surface ectoderm of the branchial pouch region. (C) Expression persists in E9.5 surface ectoderm and adjacent mesenchyme (arrowheads) of first (b1) and second branchial arch (b2), as seen in sagittal sections of whole-mount stained embryos. EphA4lacZ is a marker for cells migrating into the second and third arch of E9.0 (D) and E9.5 (E) embryos. Note the absence of label in the surface ectoderm of the second arch in E (see insert). In contrast, only low levels of EphB1 mRNA (F) and absence of EphB2lacZ protein (G) was noted on cells migrating into the arches. Expression of β-galactosidase under control of the EphB2 promoter was, however, seen in other neural crest–derived tissues such as the trigeminal ganglion (tg) and in gut endoderm forming the inner lining of pharyngeal arches (arrowheads in G). (H) EphB3-expressing cells were found to populate all three arches and the periphery of the trigeminal ganglion (tg). In transverse sections of stained embryos, ephrinB2 expression was observed in the dorsal neural tube (I) below streams of *crabp1*-positive neural crest cells (J). Complementary expression domains for ephrinB2 (K) and *crabp1* (L) were seen in the branchial arch region. Cleft between b1 and b2 has been outlined in (L). As seen in sections through the branchial arch region (cleft between b1 and b2 is shown), *crabp1*-expressing cranial neural crest cells (N) were absent in ephrinB2-expressing tissues (M, arrows in K–N).

Scale bar in (N) is 90 μm in (A), 30 μm in (B), 80 μm in (C), 120 μm in (D), 160 μm in (E)–(H) and (K)–(L), 60 μm in the insert of (E), and 40 μm in (I)–(J) and (M)–(N).

region prompted us to analyze this structure in mutant animals. In freshly dissected E9.5 (20–25 pairs of somites) wild-type or *ephrinB2*$^{WT/WT}$ embryos, three branchial arches were easily visible (Figures 4A and 4B). Interestingly, in homozygous *ephrinB2* null mutants, the second (hyoid) arch was either absent or reduced in size (34% and 55%, respectively; n = 58; Figure 4D). This defect was most prominent in the central part and less pronounced in the distal and proximal regions of the arch. In contrast, normal formation of branchial arches was observed in 92% of *ephrinB2*$^{\Delta C/\Delta C}$ homozygotes (8% reduced in size; n = 61), despite their general growth retardation, which was very similar to *ephrinB2* knockouts (Figure 4C). At this stage of development, pairwise sets of blood vessels (aortic arches) have normally formed inside each pair of the three branchial arches to direct the blood flow from the heart to the aorta. We used whole-mount immunohistochemistry with anti-PECAM1 antibodies to visualize the endothelial lining of aortic arches and other blood vessels. Stained vessels were clearly visible in the hyoid arches of control (wild type or *ephrinB2*$^{WT/WT}$) and *ephrinB2*$^{\Delta C/\Delta C}$ embryos, but completely absent in the vast majority of *ephrinB2* knockouts (91%; n = 23; Figures 4E–4H). Similar agenesis of aortic arches occurred in the proportion of *ephrinB2* knockouts, which exhibited only mild hypoplasia of hyoid arches (Figure 4H and data not shown). Furthermore, the absence of second aortic arches was confirmed in sagittal sections of embryos lacking ephrinB2 (Figure 4L). Vessel lumina were clearly visible in sectioned *ephrinB2*$^{\Delta C/\Delta C}$ and control embryos, consistent with the results of the anti-PECAM1 staining (Figures 4I–4K). Thus, the truncated ephrinB2$^{\Delta C}$ protein rescued the branchial and aortic arch defects seen in *ephrinB2* null mutants.

Early Branchial Arch and Neural Crest Formation in *ephrinB2* Mutants

We next analyzed the time course and attempted to identify possible causes for cranial defects in *ephrinB2* null mutants. At E8.5, branchial arch morphology of *ephrinB2*$^{KO/KO}$ mutants was devoid of obvious defects and appeared similar to control or *ephrinB2*$^{\Delta C/\Delta C}$ embryos. Ecto-/endodermal contact zones in the pouch region between the first and second arch were clearly visible as well as first arch arteries (Figures 5A–5C). Thus, loss of ephrinB2 seemed not to interfere with the earliest steps of branchial arch development. In the embryonic hindbrain, Eph/ephrin molecules are expressed in rhombomere-specific patterns and appear to be in-

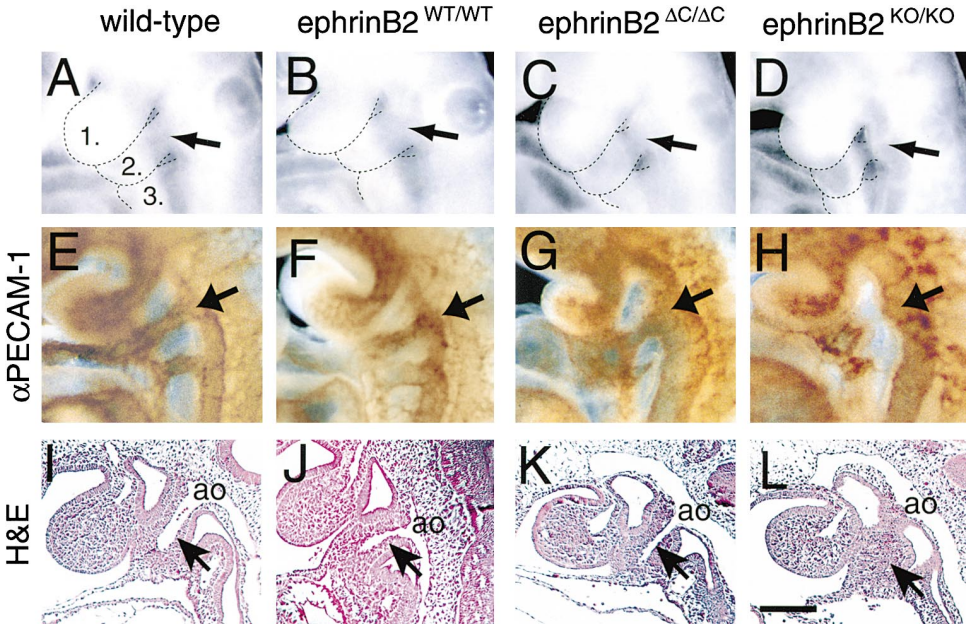

Figure 4. Hyoid Arch Defects in the *ephrinB2* Knockout Are Rescued in *ephrinB2*$^{\Delta C/\Delta C}$ Mutants

(A–D) Appearance of branchial arches in freshly dissected (A) wild-type, (B) *ephrinB2*$^{WT/WT}$, (C) *ephrinB2*$^{\Delta C/\Delta C}$, or (D) *ephrinB2*$^{KO/KO}$ embryos. Arches (1–3) were outlined by a dotted line. Note the reduction of the second branchial (hyoid) arch (arrow in D) in *ephrinB2* knockout, whereas normally developed arches can be seen in *ephrinB2*$^{\Delta C/\Delta C}$ or wild-type control animals.

(E–H) The endothelial lining of blood vessels was visualized by whole-mount immunohistochemistry with αPECAM1 (αCD31) antibody. PECAM1-positive second aortic arches were seen in wild-type, *ephrinB2*$^{WT/WT}$ and *ephrinB2*$^{\Delta C/\Delta C}$ embryos (arrows in E, F, and G), but were absent in *ephrinB2* null mutants (H).

(I–L) Sagittal sections were stained by hematoxylin and eosin. Note the absence of a vessel lumen in the hyoid arch of *ephrinB2*$^{KO/KO}$ animals (arrow in L), in contrast to matching sections through wild-type (I), *ephrinB2*$^{WT/WT}$ (J), or *ephrinB2*$^{\Delta C/\Delta C}$ (K) heads. Dorsal aorta (ao) can be seen in embryos of all four genotypes. Scale bar in (L) is 160 μm in (A)–(L).

volved in cell sorting and boundary formation (reviewed in Wilkinson, 2000). As defects in the patterning of rhombomeres could well affect cranial crest migration and branchial arch morphogenesis, we analyzed the hindbrain region of *ephrinB2* mutants by in situ hybridization with an antisense *krox20* probe (Sham et al., 1993). *Krox20* labeled rhombomeres 3 and 5 and an r5-derived stream of crest cells in *ephrinB2*$^{KO/KO}$, *ephrinB2*$^{\Delta C/\Delta C}$, and control animals, indicating that this structure developed normally in spite of partial or complete loss of ephrinB2 function (Figures 5D–5F). The homeobox gene *hoxb1* is a marker for the fourth rhombomere and streams of crest cells emerging at the r4 neural folds (Studer et al., 1998). This characteristic expression pattern was detectable in all *ephrinB2* mutant lines (Figures 5H and 5I). Expression levels in both rhombomere 4 and r4-derived crest cells, however, were reduced in *ephrinB2* null animals (Figure 5I). EphrinB2$^{\Delta C}$ was sufficient to largely, but not fully, restore *hoxb1* expression levels compared to *ephrinB2*$^{WT/WT}$ (Figures 5G and 5H) or wild-type controls (data not shown). Similar results were obtained by staining for *crabp1*: lower levels of *crabp1* expression were found in the cranial region of *ephrinB2*$^{KO/KO}$ mutants, and this reduction was most prominent for r4-derived crest (Figure 5L). Like *hoxb1* expression, *crabp1* levels were largely restored in *ephrinB2*$^{\Delta C/\Delta C}$ embryos (Figure 5K). However, the principle pattern of *crabp1*-positive cell streams emerging from rhombomere 4, as seen in *ephrinB2*$^{WT/WT}$ control animals (Figure 5J), was maintained even in *ephrinB2* null animals (Figure 5L), suggesting that the gene was not critically required for early crest migration.

Carboxyterminally Truncated EphrinB2 Is Sufficient for Guidance of Cranial Neural Crest Cells

Since cranial neural crest cells significantly contribute to mesenchyme and perhaps endothelium in the branchial arches, we followed the pathway of migrating crest cells populating this structure by whole-mount in situ hybridization with a *crabp1* antisense probe. Specific staining in wild-type embryos at E9.5 (20–25 somites) could be seen in streams of cells migrating ventrally into the arches as well as other target regions (Figure 6A). We found this late migration of *crabp1*-positive cells to be severely disrupted in *ephrinB2* null mutants. Only a few labeled cells were visible in the distal and proximal areas and the signal was even weaker in the central part of the second arch (Figure 6C). Cranial crest cells were no longer migrating in a well defined stream, were scattered, and invading adjacent areas that were normally devoid of signal in control embryos (arrowheads in Figures 6A–6C). Expression of ephrinB2 ligand lacking its cytoplasmic domain was, however, sufficient to largely restore the normal pattern of crest migration into the hyoid arch of ephrinB2$^{\Delta C/\Delta C}$ embryos (Figure 6B).

In transverse sections through the hindbrain region of whole-mount stained wild-type embryos, the stream

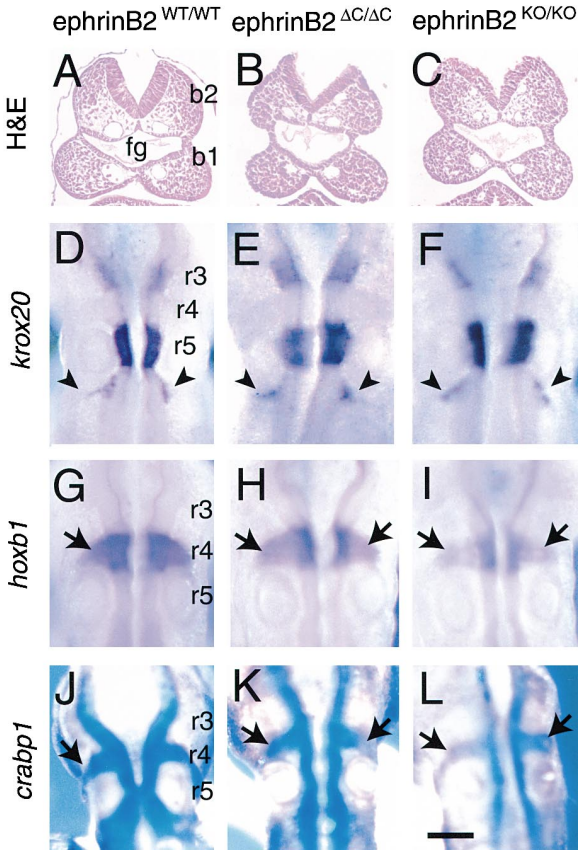

Figure 5. Early Branchial Arch and Hindbrain Morphology in *ephrinB2* Mutants

(A–C) Hematoxylin and eosin stained transverse sections through first (b1) and second branchial arch (b2) of E8.5 *ephrinB2* mutants. Normal morphology was seen in *ephrinB2*$^{WT/WT}$ (A), *ephrinB2*$^{\Delta C/\Delta C}$ (B), and *ephrinB2*$^{KO/KO}$ (C) embryos. (D–F) Whole-mount in situ hybridization of E9.5 embryos with a krox20 antisense cRNA probe. Similar staining patterns of rhombomeres r3 and r5 and crest cells emerging from r5 (arrowheads) were seen in all samples (D, E, and F). Rhombomere 4 and r4-derived crest cells expressing *hoxb1* were visualized by in situ hybridization in *ephrinB2*$^{WT/WT}$ control animals (G). Similar patterns, but reduced expression levels were seen in *ephrinB2*$^{\Delta C/\Delta C}$ (H) and most prominently in *ephrinB2*$^{KO/KO}$ (I) mutants. Likewise, *crabp1* staining of crest cells emerging from rhombomere 4 was significantly weaker in *ephrinB2* null mutants (L) compared to homozygotes expressing full-length ephrinB2 (J). Again, expression levels were largely, but not entirely restored in *ephrinB2*$^{\Delta C/\Delta C}$ mutants (K).

Scale bar in (L) is 50 μm in (A)–(C) and 100 μm in (D)–(L).

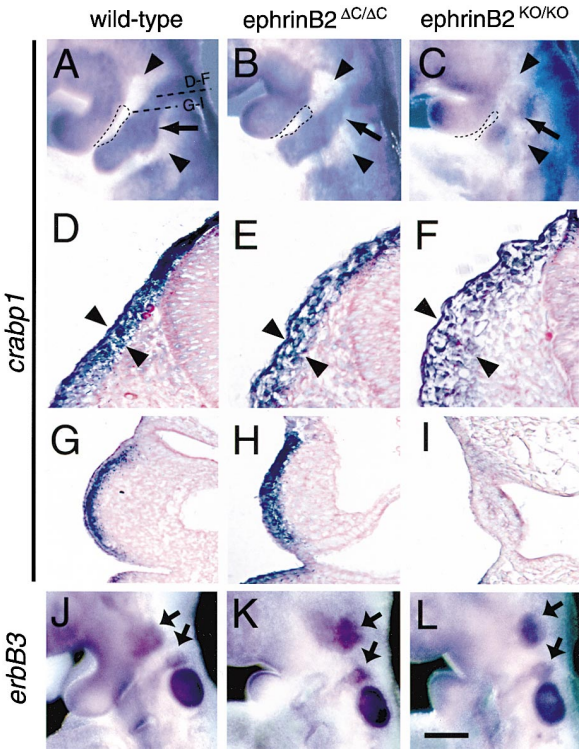

Figure 6. Cranial Neural Crest Cell Migration in *ephrinB2* Knockin Mutants

(A–I) Hindbrain and branchial arch region of E9.5 embryos stained by whole-mount in situ hybridization with an antisense *crabp1* probe that labels neural crest cells. Images of whole mounts (A–C) and transverse sections (D–I) as indicated by dotted lines in (A) are shown. A stream of crabp1-positive cranial crest cells originated at the dorsal neural tube and migrated into the second branchial arch (arrow) of (A) wild-type or (B) *ephrinB2*$^{\Delta C/\Delta C}$ animals. In *ephrinB2* knockouts, this pattern was severely disrupted and only a few labeled cells were found in the hyoid arch (C). Instead, crabp1-positive cells appeared to be scattered and invaded regions which were devoid of signal in wild-type and *ephrinB2*$^{\Delta C/\Delta C}$ embryos (arrowheads in [A]–[C]). A sharp stripe (indicated by arrowheads in [D]–[F]) of crabp1-positive crest cells was visible in sections of (D) wild-type controls and (E) *ephrinB2*$^{\Delta C/\Delta C}$ homozygotes. Loss of ephrinB2 caused this stripe to appear wider and more diffuse (F). Barely any labeled cells can be seen in transverse sections through the middle of the hypoplastic second arch (I), in contrast to (G) wild-type and (H) *ephrinB2*$^{\Delta C/\Delta C}$ arches.

(J–L) Whole-mount in situ hybridization analysis with an erbB3 antisense probe labeling neural crest cells that give rise to Schwann cells in the trigeminal ganglion and facial nerve (arrows). (J) Wild-type, (K) *ephrinB2*$^{\Delta C/\Delta C}$, and (L) *ephrinB2*$^{KO/KO}$ embryos displayed very similar staining patterns, suggesting normal migration of this cell population. Scale bar in (L) is 240 μm in (A)–(C) and (J)–(L) and 40 μm in (D)–(I).

of *crabp1*-positive crest cells migrating from the dorsal neural tube was clearly separated from adjacent tissue (Figure 6D). A similar pattern was observed in *ephrinB2*$^{\Delta C/\Delta C}$ homozygotes, although the packing of cells seemed to be not quite as compact as in control embryos (Figure 6E). In animals deficient for ephrinB2, the stripe containing labeled cells appeared much wider. The transition between labeled and unlabeled tissues was very diffuse (Figure 6F), in contrast to the sharp boundary seen in wild-type littermates. Likewise, in *ephrinB2* knockouts, barely any blue cells reached the central region of the second branchial arch, which appeared very hypoplastic in transverse sections (Figure 6I). Corresponding sections of *ephrinB2*$^{\Delta C/\Delta C}$ or wild-type embryos contained numerous crabp1-positive crest cells in close proximity of surface ectoderm (Figures 6G and 6H). Whole-mount in situ hybridization with an antisense RNA probe recognizing *erbB3*, a marker for a different population of neural crest cells, giving rise to Schwann cells of ganglia and nerves in the hindbrain region, gave similar results for *ephrinB2*$^{\Delta C/\Delta C}$, *ephrinB2* null, and control embryos (Figures 6J–6L). Blue staining was seen in trigeminal (V) and facial (VII) ganglia and

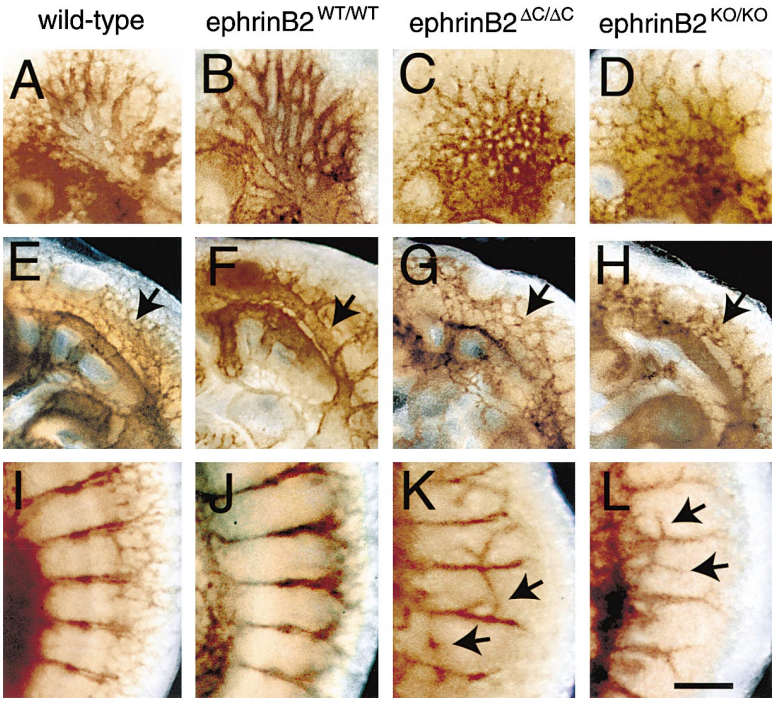

Figure 7. Blood Vessel Defects in *ephrinB2*$^{KO/KO}$ and *ephrinB2*$^{\Delta C/\Delta C}$ Embryos

(A–L) Embryonic vasculature in E9.5 embryos was visualized by whole-mount immunohistochemistry with αPECAM-1 antibody. Hierarchically organized blood vessels of different diameters can be seen in heads of wild-type (A) or *ephrinB2*$^{WT/WT}$ control embryos (B), whereas in *ephrinB2*$^{\Delta C/\Delta C}$ (C) and *ephrinB2*$^{KO/KO}$ mutants (D) the vasculature remained at the primitive capillary plexus stage. PECAM-1-stained dorsal aorta, aortic arches, and anterior cardinal vein (arrows in [E]–[H]) are normally seen in the anterior trunk region (E and F). Note defective vasculogenesis of the anterior cardinal vein in (G) *ephrinB2*$^{\Delta C/\Delta C}$ and (H) *ephrinB2* null animals. Intersomitic vessels growing in the dorsal direction (right) were not sprouting into somitic tissue of E9.5 control embryos (I and J), but disorganization of these vessels was caused by truncation (K) or loss (L) of ephrinB2. Aberrant sprouts are indicated by arrows. Scale bar in (L) is 260 μm in (A)–(D), 320 μm in (E)–(H) and 140 μm in (I)–(L).

nerves, demonstrating that the defects in *ephrinB2* null mutants were specific and did not cause a general disruption of patterning and migration in the hindbrain region.

The EphrinB2 Cytoplasmic Domain Is Required for Vascular Morphogenesis

EphrinB2 and its cognate EphB2, EphB3, and EphB4 receptors were previously shown to regulate angiogenic remodeling in the mouse embryo. At E9.5, heads of wild-type or *ephrinB2*$^{WT/WT}$ embryos contained a highly developed, hierarchically organized vascular system with large diameter blood vessels branching into smaller vessels (Figures 7A and 7B). Lack of ephrinB2 resulted in the arrest at the primitive capillary plexus stage (Figure 7D). Expression of truncated ephrinB2$^{\Delta C}$ protein did not restore angiogenic remodeling (Figure 7C). Similar defects were found for the yolk sac vasculature *of ephrinB2*$^{\Delta C/\Delta C}$ homozygotes (data not shown). In the trunk region of the embryo, major vessel primordia, such as dorsal aorta and cardinal veins, are formed by vasculogenesis. We had previously observed defects in the formation of cardinal veins in *ephrinB2* null mutants (Figure 7H) (Adams et al., 1999). As shown in Figure 7G, anterior cardinal veins did not form in *ephrinB2*$^{\Delta C/\Delta C}$ embryos. Endothelial cells were arranged in a loose, irregular network and did not form a tubular structure, resembling the phenotype of *ephrinB2* null mutants (Figure 7H). Intersomitic vessels extend from dorsal aorta and cardinal vein in a dorsal direction in a segmented pattern. In E9.5 wild-type or *ephrinB2*$^{WT/WT}$ embryos, these vessels were found to respect somitic boundaries by not forming endothelial sprouts penetrating into somites (Figures 7I and 7J). In contrast, numerous aberrant branches and sprouts invaded somitic tissue in both *ephrinB2*$^{\Delta C/\Delta C}$ and *ephrinB2*$^{KO/KO}$ mutants (Figures 7K and 7L) (Adams et al., 1999). These findings provide genetic proof that ephrinB2 requires a cytoplasmic domain to mediate vascular morphogenesis during mouse embryogenesis. They further suggest that ephrinB2 reverse signaling or other functions mediated by the cytoplasmic domain in addition to EphB receptor forward signaling may be important for this process.

In Vitro Endothelial Sprouting Is Induced by EphB-Fc, Suggestive of EphrinB Reverse Signaling

Using an in vitro sprouting assay as a correlate of in vivo sprouting angiogenesis, we had previously demonstrated that ephrinB1 and ephrinB2 ligands had stimulatory influences on capillary sprouting of adrenal cortex–derived microvascular endothelial (ACE) cells (Adams et al., 1999). Having observed an in vivo requirement for the ephrinB2 cytoplasmic domain, we reasoned that stimulating endogenous ephrinB ligands with EphB soluble ectodomains might induce in vitro sprouting. Purified EphB3-Fc and EphB4-Fc fusion proteins induced a significant, dose-dependent increase in the number of sprouts with a length exceeding the diameter of the bead (Figure 8). In contrast, EphB2-Fc (this study) and EphB1-Fc (Adams et al., 1999) were not effective in this assay, suggesting a certain degree of functional specificity of the response. Differences in sprout inducing activity may be due to different binding kinetics. Highest affinities toward ephrinB2 were measured with EphB3 and EphB4 receptors, compared to EphB1 and EphB2 (for review, see Flanagan and Vanderhaeghen, 1998). These results indicate that in vitro endothelial sprouting can be mediated by ephrinB stimulation and presumably reverse signaling and provide strong support for the concept that this process is required for vascular morphogenesis in vivo.

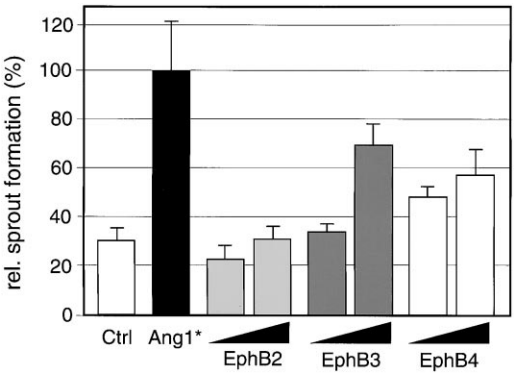

Figure 8. EphrinB-Mediated Angiogenic Sprouting In Vitro

Adrenal-cortex-derived microvascular endothelial cells (ACE) were cultured on beads in three-dimensional fibrin gels. Following 2 days of incubation, endothelial sprouts exceeding the diameter of the bead were quantified and normalized relative to basal sprouting activity in the absence of angiogenic factors (Control). Endothelial sprouting was induced by incorporation of dimeric EphB3-Fc or EphB4-Fc, but not EphB2-Fc fusion proteins (0.22 and 1 μg/ml) into the fibrin matrix. Saturating amounts (0.67 μg/ml) of recombinant angiopoietin-1 (Ang1*) were used as positive control.

Reduced Tie2 and Angiopoietin-1 Expression in *ephrinB2* Mutants

We next introduced a *tie2-lacZ* reporter transgene (Schlaeger et al., 1997) into our *ephrinB2* allelic series to use endothelial-specific expression of β-galactosidase as an independent marker for vascular morphogenesis. As observed by anti-PECAM1 immunohistochemistry, both *ephrinB2*$^{KO/KO}$ and *ephrinB*$^{\Delta C/\Delta C}$ embryos showed β-galactosidase positive endothelial cells arrested at the capillary plexus stage (Figures 9B and 9C). Surprisingly, the expression of β-galactosidase from a single allele of the *tie2-lacZ* transgene was greatly reduced in both mutants compared to wild-type (Figure 9A) or *ephrinB2*$^{WT/WT}$ control animals (data not shown). Reduced expression of the endogenous *tie2* gene in *ephrinB2*$^{KO/KO}$ and *ephrinB*$^{\Delta C/\Delta C}$ embryos was confirmed by whole-mount immunohistochemistry using anti-Tie2 antibodies (Figures 9E and 9F). In contrast, expression of vascular endothelial growth factor receptor-2 (VEGFR2) was unaffected in ephrinB2 mutants (Figures 9H and 9I). We next determined the levels of *Tie2* mRNA by semiquantitative RT-PCR analysis using GAPDH as reference. It was confirmed that the levels of *VEGFR2* mRNA were unchanged in both ephrinB2 mutants. In contrast, the levels of *tie2* mRNA and its cognate ligand *angiopoietin-1* (*Ang1*) were significantly reduced relative to *VEGFR2* mRNA (Figures 9J and 9K) or *VEGFR1*, *VEGF*, *Tie1*, *Ang2*, *VE-Cadherin*, and *PECAM-1* mRNAs (data not shown). Ang1 is normally produced by support cells, while Tie2 receptors are expressed by endothelial cells. The fact that *Ang1* expression is reduced in *ephrinB2*$^{KO/KO}$ and *ephrinB*$^{\Delta C/\Delta C}$ mutants suggests a requirement for ephrin/Eph bidirectional signaling in endothelial/mesenchymal cell interactions.

Discussion

In this study, we present genetic evidence that ephrinB2 exerts a dual role in mouse development. Besides being an important regulator of vascular development (Wang et al., 1998; Adams et al., 1999), ephrinB2 is essential for branchial arch morphogenesis. We further demonstrate that in order to mediate angiogenic remodeling, ephrinB2 requires its highly conserved cytoplasmic domain. In vitro, angiogenic sprouting can be induced by soluble EphB-Fc receptor bodies, suggesting that ephrinB can indeed have receptor-like signaling properties. Together, these results emphasize the importance of the cytoplasmic domain of transmembrane ephrins, presumably to mediate reverse signaling in vascular morphogenesis. In contrast, carboxyterminally truncated ephrinB2 rescues the migration defect of branchial neural crest cells, suggesting that forward signaling via EphB receptors in crest cells is sufficient for this process. Finally, we show that expression of carboxyterminally truncated ephrinB2 results in downregulation of *Ang1* expression in mesenchymal cells, implying that reverse ephrin or bidirectional ephrin/Eph signaling is required for proper communication between endothelial and mesenchymal cells.

A potential caveat is raised by the discovery that, in solution, higher-order clustering of ephrins is required for full activation of Eph receptors. Because clustering of transmembrane ephrins may be mediated by the cytoplasmic domain through interaction with intracellular proteins, it is possible that the ephrinB2$^{\Delta C}$ mutant may not be fully functional in triggering Eph receptor forward signaling. Several observations make this interpretation rather unlikely. Ephrins and Eph receptors restrict cell intermingling across hindbrain segment boundaries. It was shown that ectopically expressed truncated ephrins are sufficient for cell sorting toward rhombomere boundaries (Xu et al., 1999). Truncated ephrinB2 was also sufficient to restrict communication between cells via gap junctions and to restrict cell intermingling in a zebrafish animal cap assay (Mellitzer et al., 1999). In our system, truncated ephrinB2$^{\Delta C}$ rescues branchial arch morphogenesis, but not angiogenesis. If lack of Eph receptor activation due to insufficient ephrin clustering caused the angiogenesis defect, one would have to argue that the mechanism of ephrin clustering is different in branchial arch ectoderm/mesenchyme and endothelial cells. However, there is currently no evidence in favor of such differential mechanisms. Previous work has also demonstrated that ephrinB1, a homolog of ephrinB2, can be located in sphingolipid/cholesterol-enriched raft membrane microdomains, which was not the case for a carboxyterminally truncated version of the ligand (Brückner et al., 1999). Potential alterations in plasma membrane microdomain localization are apparently not affecting gap junction formation and reconstituted bidirectional signaling in a zebrafish animal cap assay (Mellitzer et al., 1999) or guidance of cranial crest cells in vivo (this study). Therefore, truncated ephrinB2$^{\Delta C}$ appears capable of triggering Eph receptor forward signaling, but incapable of triggering reverse signaling, via its cytoplasmic tail. We therefore demonstrate distinct requirements for morphogenetic functions mediated by the ephrinB2 extracellular and cytoplasmic domains, respectively.

Previous studies have addressed the role of ephrin/Eph molecules in guidance of neural crest cells of vertebrate embryos. Several EphA and EphB receptors were

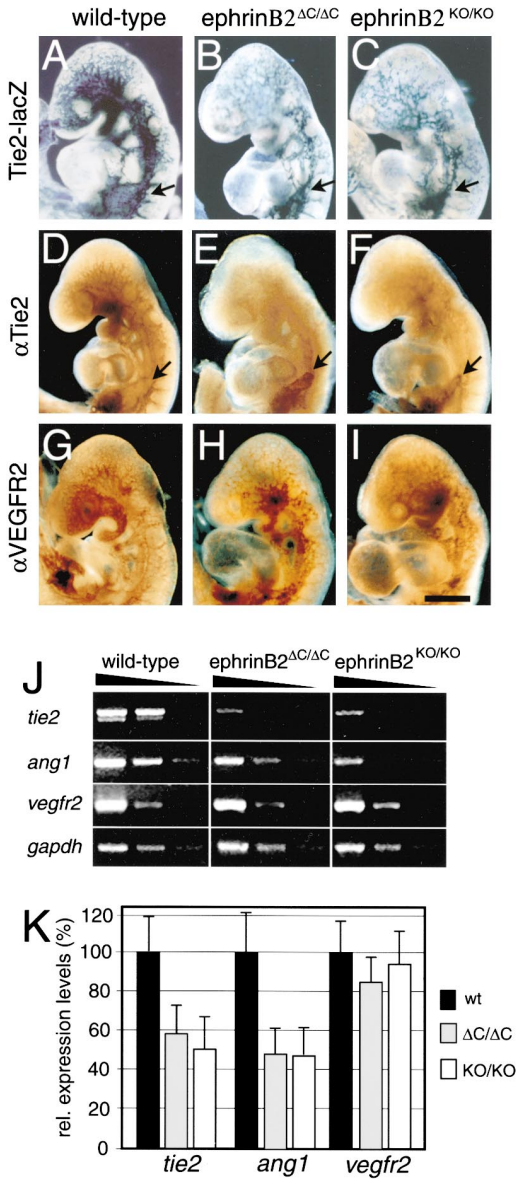

Figure 9. Reduced Expression of Tie2 and Angiopoietin-1 in *ephrinB2* Mutants

(A–C) Expression of β-galactosidase under control of the Tie2 promoter (Tie2-lacZ) gave a strong endothelial cell-specific staining in E9.5 wild-type embryos (A), but was reduced in (B) *ephrinB2*$^{\Delta C/\Delta C}$ or (C) *ephrinB2*$^{KO/KO}$ mutants processed in parallel. Normal lacZ reporter expression was seen in part of the cardinal vein close to the sinus venosus (arrows in [B] and [C]).

(D–F) Whole-mount immunohistochemistry with αTie2 antibody. Vascular staining in E9.5 (E) *ephrinB2*$^{\Delta C/\Delta C}$ or (F) *ephrinB2*$^{KO/KO}$ mutants was reduced compared to control littermates (D). Note Tie2 staining close to the sinus venous (arrows in [E] and [F]) resembling lacZ results. In contrast, similar staining levels were obtained with αVEGFR2 antibody for (G) wild-type, (H) *ephrinB2*$^{\Delta C/\Delta C}$, and (I) ephrinB2 knockout embryos. (J) Ethidium bromide–stained amplification products of semiquantitative RT-PCR with Tie2-, Ang1-, VEGFR2-, and GAPDH-specific primer pairs are shown. Different dilutions of single-stranded cDNA (1:1, 1:5, and 1:25, see Supplemental Data indicated in the Experimental Procedures) prepared from E9.5 wild-type, *ephrinB2*$^{\Delta C/\Delta C}$, or *ephrinB2*$^{KO/KO}$ embryos (n = 7 for each genotype) were used. Levels of Tie2 and Ang1 mRNA were reduced in ephrinB2 mutants. (K) Relative intensity levels of SYBR green stained PCR products were measured in a phosphoimager and normalized for GAPDH levels. No significant alteration of VEGFR2-specific product was seen. Scale bar in (I) is 400 μm in (A)–(I).

shown to be expressed on cranial neural crest (CNC) cells populating third and fourth branchial arches in *Xenopus laevis*. Contrary to the mouse, ephrinB2 was found in adjacent second arch neural crest and mesoderm (Smith et al., 1997; Helbling et al., 2000). RNA injection and overexpression of ephrinB2 or truncated EphA4 or EphB1 receptors induced scattering of CNC cells into adjacent regions in *Xenopus* embryos (Smith et al., 1997). The phenotype was very similar to *ephrinB2* null mutant mice described in this study, in spite of species-specific differences in expression patterns. In the embryonic trunk region, EphB receptor-expressing crest cells in vitro avoided substrate stripes containing recombinant ephrinB1- or ephrinB2-Fc protein (Krull et al., 1997; Wang and Anderson, 1997). A repulsive mechanism, similar to axonal growth cone pathfinding, leading to the characteristic segmental rostrocaudal pattern of migrating crest was suggested by both studies. Similarities in the expression of Eph receptors, found on CNC cells, and ephrinB2, in branchial arches, make it attractive to postulate that a repulsive mechanism might also be operating for crest guidance in embryonic heads.

Our analysis of hindbrain patterning and CNC morphogenesis in ephrinB2 mutants revealed downregulation of markers for r4-derived crest cells. In contrast, no alterations were seen for krox20-positive cells emerging from rhombomere 5. What might be the function of ephrinB2 in this early step of cranial crest morphogenesis and how can it be specific for one CNC subpopulation but not for another? Neural crest cells delaminate from the neuroectoderm at the epidermal–neural plate interface before they migrate toward their target sites. Soluble factors, such as Bmp2, secreted by the surface ectoderm, are required for the induction of crest cells and maintenance of their cell fate (Kanzler et al., 2000). Remarkably, blocking of Bmp2/4 function by transgenic noggin expression or inactivation of the Bmp2 gene caused defects in formation and/or migration of crabp1-positive cranial crest cells (Kanzler et al. 2000), a phenotype that resembles defects seen in *ephrinB2* null mutants. Thus, ephrinB2, expressed by the dorsal neural ectoderm, might be involved in cranial neural crest delamination and migration out of the neuroepithelium, presumably by providing a repulsive signal. Expression of ephrinB2 in the E8.5/E9.5 hindbrain is specific for even-numbered rhombomeres, which might explain why r4- but not r5-derived crest cells are affected. Levels of *hoxb1* and *crabp1* signals and CNC development appear to be largely restored in *ephrinB*$^{\Delta C/\Delta C}$ mutants, indicating that the ephrinB2 cytoplasmic domain is not critically required for this process. The slight reduction of marker expression in *ephrinB*$^{\Delta C/\Delta C}$ mutants might indicate a minor contribution of the carboxyterminal domain or simply result from the general growth retardation caused by vascular defects.

Which receptors are candidates for mediating the ephrinB2 signal in neural crest cells? *EphA4* null mutants displayed defects in guidance of motor nerves and for-

mation of the corticospinal tract (reviewed in Wilkinson, 2000; see also Helmbacher et al., 2000; Kullander et al., 2001), but had no overt phenotype affecting migration of neural crest cells or development of crest-derived tissues. Likewise, *ephB2* and *ephB3* null animals regulate brain commissure formation (Henkemeyer et al., 1996; Orioli et al., 1996), but not crest cell guidance (Wang and Anderson, 1997). The penetrance of commissure agenesis was increased and additional defects were observed in *ephB2/ephB3* double mutants, indicating functional redundancy between the two receptors (Orioli et al., 1996; Adams et al., 1999). Loss of EphB4 resulted in vascular malformations highly reminiscent of *ephrinB2* mutants (Gerety et al., 1999). Based on staining with a lacZ reporter, EphB4 is not expressed in hindbrain or branchial arches (Gerety et al., 1999). Thus, it appears that redundant activity of multiple Eph receptors, including EphA4, EphB1, and EphB3, on cranial crest cells might mediate ephrinB2-dependent guidance.

The cytoplasmic domain of ephrinB, i.e., reverse signaling, appears to be important for the communication between endothelial/periendothelial cells, but not between branchial arch ectoderm/mesenchyme and neural crest cells. The reason for this difference is currently unknown. Angiogenic remodeling is a complex process which requires endothelial cells to de-adhere from one another and from the substratum, to migrate, divide, and form tubular structures. Endothelial cells coexpress certain ephrin ligands and Eph receptors, which might impact on many of the cellular responses during angiogenic remodeling. The arterial–venous interface appears to be a prominent site of ephrin/Eph interaction, since ephrinB2 and EphB4 molecules are predominantly expressed on arteries and veins, respectively, and *ephrinB2* and *ephB4* mutant mice display similar vascular defects. The apparent mutual interdependence of their interaction has thus far precluded discrimination between uni- and bidirectional signaling between ephrinB2 and EphB4. Further insight is now provided by our study, indicating that the ephrinB2 carboxyterminal domain and its interaction with putative cytoplasmic proteins is indispensable for angiogenic remodeling. Our study, however, does not demonstrate a requirement for EphB4 kinase activity, i.e., forward signaling, in the vascular system. A reciprocal genetic approach, the generation of mutant mice expressing a kinase-dead EphB4 receptor, will allow that question to be addressed.

Evidence for simultaneous signal transduction both downstream of EphB4 and ephrinB2 came from in vitro data. Either activation of EphB receptors by ephrinB-Fc fusion proteins (Adams et al., 1999) or activation of ephrinB ligands by EphB3-Fc or EphB4-Fc fusion proteins is sufficient to induce endothelial sprouting in vitro (this study). Thus, both means of stimulation should occur in parallel between endothelial cells coexpressing ligands and receptors. What might be the precise role of ephrin/Eph signaling in the vasculature and which mechanism is underlying the defects in *ephrinB2, ephB4* null, and *ephrinB*$^{\Delta C/\Delta C}$ mutants? An answer might be provided by several other loss-of-function mouse mutants. Targeted inactivation of the adhesion molecule VE-Cadherin (Carmeliet et al., 1999), the transcription factor COUP-TFII (Pereira et al., 1999), Ang-1 (Suri et al., 1996) and its receptor, Tie2 (Dumont et al., 1994) resulted in midgestational lethality with similar vascular phenotypes. These phenotypes may be the result of disrupted cell–cell communication in the vascular system by different, independent defects. Alternatively, these molecules may represent parts of the same signaling cascade. Indeed, reduced Ang-1 mRNA levels were reported for *COUP-TFII* mutant animals, suggesting a direct or indirect connection between the transcription factor COUP-TFII and the soluble ligand Ang-1 (Pereira et al., 1999). In the present study, the expression of both Ang-1 and Tie2 were specifically reduced in *ephrinB2* mutant animals, whereas numerous other vascular markers were not significantly altered. No reduction of *Tie2* expression was found in *VE-Cadherin* null animals (Carmeliet et al., 1999), indicating that its downregulation is not a general result of vascular malformation. It therefore is conceivable that the phenotypic similarities of *ephrinB2/ephB4* and *ang-1/tie2* mutants are a consequence of transcriptional downregulation. Since endothelial cells coexpress ephrin/Eph molecules and Tie2, expression of Tie2 might be under control of ephrinB2 reverse or bidirectional signaling. Mesenchymal cells in the proximity of blood vessels and capillaries are the site of Ang-1 expression, which might be controlled by ephrinB2 interaction with Eph receptors present on mesenchymal cells. Alternatively, an indirect mechanism, e.g., via a soluble factor secreted by endothelial cells that acts on mesenchyme, appears equally feasible. Regardless of these different mechanisms, downregulation of the Ang1/Tie2 system may be the primary cause for the observed vascular defects in *ephrinB2* mutants. In addition, the activity of both ephrinB and EphB molecules in sprouting assays in vitro suggests direct roles in vascular remodeling independent of the Ang1/Tie2 system.

Experimental Procedures

Please refer to supplementary online information for details (http://www.cell.com/cgi/content/full/104/1/57/DC1).

Generation of Mutant Mice

The generation of a replacement-type targeting vector for *ephrinB2* was described previously (Adams et al., 1999). Here, cDNAs encoding either mouse wild-type (ephrinB2^{wt}) or C terminally truncated ephrinB2 (ephrinB2$^{\Delta C}$, amino acid residues 1–267, corresponding to peptide sequence MARS...HTTT) were fused in frame to exon1. For protein detection, a hemagglutinin (HA) epitope tag was added at the ephrinB2$^{\Delta C}$ carboxyterminus (...HTTT/MYPYDVPDYASL*).

RT-PCR Analysis

Total RNA was isolated from E9.5 mutant and control embryos using TRIZOL reagent (GibcoBRL) according to the manufacturer's instructions, digested with DNAse, and subjected to reverse transcription. Single-stranded cDNA was used for PCR amplification according to standard protocols to detect expression of endogenous ephrinB2 or ephrinB2^{wt} and ephrinB2$^{\Delta C}$ mRNAs. For semiquantitative RT-PCR analysis, 0.5 μl of reverse transcription reaction was either used directly or in 1:5, 1:25, 1:50, or 1:100 dilution for amplification (33 cycles) with gene-specific primers. After separation in 1.5% agarose gels, PCR products were stained with 10 μg/ml ethidium bromide solution (for pictures shown in Figure 1 and 8) or with SYBR Green Nucleic Acid Gel Stain (Roche). SYBR Green stained products were quantified using a Fuji FLA-2000 scanner (Aida 2.0 software) and normalized for GAPDH expression. Linear relationship was observed for amplification results from different dilutions indicating non-saturating PCR conditions.

Wheat Germ Agglutinin Pull Down, Immunoprecipitation, and Western Blotting

Glycosylated proteins in embryo lysates were enriched by pull-down with sepharose-coupled Triticum vulgaris lectin (Sigma, L6257). For EphB4 stimulation experiments, cultured HUVECs (60% confluent) were treated with membranes obtained from ephrinB2^{WT}, ephrinB2$^{\Delta C}$ or empty vector (mock) transfected HEK293 cells or IgG Fc fusion proteins and analyzed by immunoprecipitation. Samples from pull-down or immunoprecipitation experiments were analyzed by SDS-PAGE/immunoblotting with antibodies specific for ephrinB2 (R&D Systems, AF496), HA-epitope tag (Babco, PRB-101C), phosphotyrosine (Upstate Biotechnology, clone 4g10), or EphB4 receptor and developed using secondary HRP-coupled antibodies (Amersham) and ECL Western Blotting Detection Reagent (Amersham).

Whole-Mount Staining with Alkaline Phosphatase Fusion Proteins

Freshly dissected E9.5 embryos were washed three times with ice-cold PBS (5 min each) and blocked in DMEM, 10% calf serum, and 0.1% NaN_3 for 30 min. Incubation with fusion protein (10 nM) of EphB4 receptor extracellular domain and human secreted alkaline phosphatase in blocking solution was done overnight (at 4°C) followed by washing, heat inactivation of endogenous phosphatases, and color development as described previously (Adams et al., 1999).

Whole-Mount Immunohistochemistry, lacZ Staining, and In Situ Hybridization

Embryos were fixed with 4% PFA and stained with primary monoclonal antibodies against PECAM-1 (Pharmingen, clone MEC13.3, isotype rat, 1:50 dilution), Tie2 (clone 4g8, isotype rat, 1:25), or VEGFR2 (clone 12β11, isotype rat, 1:50) and secondary antibodies against rat IgG, and avidin-conjugated peroxidase (Rat IgG VECTASTAIN ABC Kit). β-galactosidase staining of whole embryos, generation of digoygenin-labeled antisense riboprobes, pretreatment and in situ hybridization of E9.5 embryos, and sectioning of stained embryos were described previously (Henkemeyer et al., 1996; Adams et al., 1999).

In Vitro Sprouting Angiogenesis Assay

The assay and generation of Ang1* was described (Koblizek et al., 1998). Purified fusion proteins of Eph receptor extracellular domains and human immunoglobulin Fc region (R&D Systems) were used at concentrations of 0.22 and 1.0 μg/ml without clustering by antibodies.

Acknowledgments

We thank K. Vintersten of the Transgenic Service and the staff of the EMBL Laboratory Animal Resources for generation of chimeric mice and expert support, S. Adams and the laboratory of P. Angel for technical help, H. Augustin for communicating unpublished data, and J. Wittbrodt and K. Kullander for critically reading the manuscript. EphA4lacZ mice, HUVECs, EphB4 antiserum, and templates for RNA probes were gifts from P. Charnay, B. Kraeling, A. Ziemiecki, E. N. Olson, M. Gassmann, M. Maden, and I. Grunwald; purified Ang1* and IgG Fc were provided by G. D. Yancopoulos, Regeneron Pharmaceuticals Inc. Support for this study came in part from the Deutsche Forschungsgemeinschaft (DFG,KL948/4-1 and SFB488) to R. K.

Received June 19, 2000; revised December 8, 2000.

References

Adams, R.H., Wilkinson, G.A., Weiss, C., Diella, F., Gale, N.W., Deutsch, U., Risau, W., and Klein, R. (1999). Roles of ephrinB ligands and EphB receptors in cardiovascular development: demarcation of arterial/venous domains, vascular morphogenesis and sprouting angiogenesis. Genes Dev. *13*, 295–306.

Brückner, K., Labrador, J.P., Scheiffele, P., Herb, A., Bradke, F., Seeburg, P.H., and Klein, R. (1999). EphrinB ligands recruit GRIP family PDZ adaptor proteins into raft membrane microdomains. Neuron *22*, 511–524.

Carmeliet, P., Lampugnani, M.G., Moons, L., Breviario, F., Compernolle, V., Bono, F., Balconi, G., Spagnuolo, R., Oostuyse, B., Dewerchin, M., et al. (1999). Targeted deficiency or cytosolic truncation of the VE-cadherin gene in mice impairs VEGF-mediated endothelial survival and angiogenesis. Cell *98*, 147–157.

Davy, A., Gale, N.W., Murray, E.W., Klinghoffer, R.A., Soriano, P., Feuerstein, C., and Robbins, S.M. (1999). Compartmentalized signaling by GPI-anchored ephrin-A5 requires the Fyn tyrosine kinase to regulate cellular adhesion. Genes Dev. *13*, 3125–3135.

Dumont, D.J., Gradwohl, G., Fong, G.H., Puri, M.C., Gertsenstein, M., Auerbach, A., and Breitman, M. (1994). Dominant-negative and targeted null mutations in the endothelial receptor tyrosine kinase, tek, reveal a critical role in vasculogenesis of the embryo. Genes Dev. *8*, 1897–1909.

Flanagan, J.G., and Vanderhaeghen, P. (1998). The ephrins and Eph receptors in neural development. Annu. Rev. Neurosci. *21*, 309–345.

Gale, N.W., and Yancopoulos, G.D. (1999). Growth factors acting via endothelial cell-specific receptor tyrosine kinases: VEGFs, angiopoietins, and ephrins in vascular development. Genes Dev. *13*, 1055–1066.

Gerety, S.S., Wang, H.U., Chen, Z.F., and Anderson, D.J. (1999). Symmetrical mutant phenotypes of the receptor EphB4 and its specific transmembrane ligand ephrinB2 in cardiovascular development. Mol. Cell *4*, 403–414.

Helbling, P.M., Saulnier, D.M., and Brändli, A.W. (2000). The receptor tyrosine kinase EphB4 and ephrin-B ligands restrict angiogenic growth of embryonic veins in Xenopus laevis. Development *127*, 269–278.

Helmbacher, F., Schneider-Maunoury, S., Topilko, P., Tiret, L., and Charnay, P. (2000). Targeting of the EphA4 tyrosine kinase receptor affects dorsal/ventral pathfinding of limb motor axons. Development *127*, 3313–3324.

Henkemeyer, M., Orioli, D., Henderson, J.T., Saxton, T.M., Roder, J., Pawson, T., and Klein, R. (1996). Nuk controls pathfinding of commissural axons in the mammalian central nervous sustem. Cell *86*, 35–46.

Holder, N., and Klein, R. (1999). Eph receptors and ephrins: effectors of morphogenesis. Development *126*, 2033–2044.

Kanzler, B., Foreman, R.K., Labosky, P.A., and Mallo, M. (2000). BMP signaling is essential for development of skeletogenic and neurogenic cranial neural crest. Development *127*, 1095–1104.

Koblizek, T.I., Weiss, C., Yancopoulos, G.D., Deutsch, U., and Risau, W. (1998). Angiopoietin-1 induces sprouting angiogenesis in vitro. Curr. Biol. *8*, 529–532.

Kontges, G., and Lumsden, A. (1996). Rhombencephalic neural crest segmentation is preserved throughout craniofacial ontogeny. Development *122*, 3229–3242.

Krull, C.E., Lansford, R., Gale, N.W., Collazo, A., Marcelle, C., Yancopoulos, G.D., Fraser, S.E., and Bronner-Fraser, M. (1997). Interactions of Eph-related receptors and ligands confer rostrocaudal pattern to trunk neural crest migration. Curr. Biol. *7*, 571–580.

Kullander, K., Mather, N.K., Diella, F., Dottori, M., Boyd, A.W., and Klein, R. (2001). Kinase-dependent and kinase-independent functions of EphA4 receptors in major axon tract formation in vivo. Neuron, in press.

Maden, M., Horton, C., Graham, A., Leonard, L., Pizzey, J., Siegenthaler, G., Lumsden, A., and Eriksson, U. (1992). Domains of cellular retinoic acid-binding protein I (CRABP I) expression in the hindbrain and neural crest of the mouse embryo. Mech. Dev. *37*, 13–23.

Mellitzer, G., Xu, Q., and Wilkinson, D.G. (1999). Eph receptors and ephrins restrict cell intermingling and communication. Nature *400*, 77–81.

Orioli, D., Henkemeyer, M., Lemke, G., Klein, R., and Pawson, T. (1996). Sek4 and Nuk receptors cooperate in guidance of commissural axons and in palate formation. EMBO J. *15*, 6035–6049.

Pereira, F.A., Qiu, Y., Zhou, G., Tsai, M.J., and Tsai, S. (1999). The orphan nuclear receptor COUP-TFII is required for angiogenesis and heart development. Genes Dev. *13*, 1037–1049.

Schlaeger, T.M., Bartunkova, S., Lawitts, J.A., Teichmann, G., Risau,

W., Deutsch, U., and Sato, T.N. (1997). Uniform vascular-endothelial-cell-specific gene expression in both embryonic and adult transgenic mice. Proc. Natl. Acad. Sci. USA *94*, 3058–3063.

Sham, M.H., Vesque, C., Nonchev, S., Marshall, H., Frain, M., Gupta, R.D., Whiting, J., Wilkinson, D., Charnay, P., and Krumlauf, R. (1993). The zinc finger gene Krox20 regulates HoxB2 (Hox2.8) during hindbrain segmentation. Cell *72*, 183–196.

Smith, A., Robinson, V., Patel, K., and Wilkinson, D.G. (1997). The EphA4 and EphB1 receptor tyrosine kinases and ephrin-B2 ligand regulate targeted migration of branchial neural crest cells. Curr. Biol. *7*, 561–570.

Studer, M., Gavalas, A., Marshall, H., Ariza-McNaughton, L., Rijli, F.M., Chambon, P., and Krumlauf, R. (1998). Genetic interactions between Hoxa1 and Hoxb1 reveal new roles in regulation of early hindbrain patterning. Development *125*, 1025–1036.

Suri, C., Jones, P.F., Patan, S., Bartunkova, S., Maisonpierre, P.C., Davis, S., Sato, T.N., and Yancopoulos, G.D. (1996). Requisite role of angiopoietin-1, a ligand for the TIE2 receptor, during embryonic angiogenesis. Cell *87*, 1171–1180.

Wang, H.U., and Anderson, D.J. (1997). Eph family transmembrane ligands can mediate repulsive guidance of trunk neural crest migration and motor axon outgrowth. Neuron *18*, 383–396.

Wang, H.U., Chen, Z.-F., and Anderson, D.J. (1998). Molecular Distinction and Angiogenic Interaction between Embryonic Arteries and Veins Revealed by ephrin-B2 and Its Receptor Eph-B4. Cell *93*, 741–753.

Wilkinson, D.G. (2000). Eph receptors and ephrins: regulators of guidance and assembly. Int. Rev. Cytol. *196*, 177–244.

Xu, Q., Mellitzer, G., Robinson, V., and Wilkinson, D.G. (1999). In vivo cell sorting in complementary segmental domains mediated by Eph receptors and ephrins. Nature *399*, 267–271.